On some constitutive equations for micropolar plates

Jacek Chróścielewski, Wojciech Witkowski*

Gdansk University of Technology,

Faculty of Civil and Environmental Engineering, Department of Structural Mechanics and Bridge Structures

80-233 Gdańsk, Narutowicza 11/12, Poland

*corresponding author

wojwit@pg.gda.pl

Abstract

In this paper we discuss the constitutive relations for micropolar plates recently obtained by Altenbach and Eremeyev. We pay particular attention to their relation for the resultant drilling stress couple and compare it with that used so far in the statically and kinematically exact nonlinear six-parameter shell theory. Using the results of Altenbach and Eremeyev, we present bounds on values of the constitutive parameter α_t from the six-parameter shell theory model. Some representative numerical simulations show how the drilling stiffness α_t affects the FEM results.

1. Introduction

In an interesting paper [1] pursued an important problem of constitutive relations for micropolar plates. While the kinematics of the micropolar continuum is rather well-described (see for instance [2] and references given there) the problem of corresponding material laws is still discussed in the literature. Some of the recent advances concerning micropolar hyperelasticity in planar case may be found e.g. in [3] and references given therein.

Altenbach and Eremeyev [1] obtained their governing equations using the direct approach. They compare the constitutive relations of micropolar plate with the constitutive equations used in the six-parameter nonlinear theory of shells (referred here as the shell constitutive equations) used, among others, in [5-9]. Particularly interesting seems to be the constitutive relation for the drilling couple resultant.

The aim of this study is to discuss the comparison further. The principal assumption of this paper is that the constitutive model from [1] is equivalent to shell constitutive equations from e.g. [5-9].

We express the shell constitutive equations in terms of those proposed in [1]. We discuss the conditions of equivalence between these two models and show relations between the material constants. Finally, we present some representative numerical examples associated with constitutive relation for the resultant drilling stress couple and discuss how values of the constitutive parameter α_t may affect the FEM numerical results. In particular we introduce the notion 'α_t-locking' to describe the situations where, in membrane dominated deformations, large values of α_t cause too stiff responses in FEM analysis.

2. Comparison

2.1. General remarks

Throughout the text an equation number preceded by AE designates the respective equation from the source paper [1].

Equation AE11 defines the surface strain energy density of an isotropic micropolar plate. The constitutive equations for the force tensor and the moment tensor components follow then from AE12 and AE13, respectively. Rewriting equations AE12 and AE13 in matrix form (see Appendix 1 of this paper) leads to

$$
\begin{bmatrix}
N^{11} \\
N^{22} \\
N^{12} \\
N^{21} \\
Q^{1} \\
Q^{2} \\
M^{11} \\
M^{22} \\
M^{12} \\
M^{21} \\
M^{1} \\
M^{2}
\end{bmatrix}
=
\left[
\begin{array}{cccccc|cccccc}
\alpha_1+\alpha_2+\alpha_3 & \alpha_1 & 0 & 0 & 0 & 0 & & & & & & \\
\alpha_1 & \alpha_1+\alpha_2+\alpha_3 & 0 & 0 & 0 & 0 & & & & & & \\
0 & 0 & \alpha_3 & \alpha_2 & 0 & 0 & & & & & & \\
0 & 0 & \alpha_2 & \alpha_3 & 0 & 0 & & & & & & \\
0 & 0 & 0 & 0 & \alpha_4 & 0 & & & & & & \\
0 & 0 & 0 & 0 & 0 & \alpha_4 & & & & & & \\
\hline
& & & & & & \beta_1+\beta_2+\beta_3 & \beta_1 & 0 & 0 & 0 & 0 \\
& & & & & & \beta_1 & \beta_1+\beta_2+\beta_3 & 0 & 0 & 0 & 0 \\
& & & & & & 0 & 0 & \beta_3 & \beta_2 & 0 & 0 \\
& & & & & & 0 & 0 & \beta_2 & \beta_3 & 0 & 0 \\
& & & & & & 0 & 0 & 0 & 0 & \beta_4 & 0 \\
& & & & & & 0 & 0 & 0 & 0 & 0 & \beta_4
\end{array}
\right]
\begin{bmatrix}
\varepsilon_{11} \\
\varepsilon_{22} \\
\varepsilon_{12} \\
\varepsilon_{21} \\
\varepsilon_{1} \\
\varepsilon_{2} \\
\kappa_{11} \\
\kappa_{22} \\
\kappa_{12} \\
\kappa_{21} \\
\kappa_{1} \\
\kappa_{2}
\end{bmatrix}
\tag{1}
$$

Two blocks of equation (1) are written in notations used in [5-8] i.e. in terms of components of the strain vector ($\varepsilon_{\alpha\beta}, \varepsilon_\alpha, \kappa_{\alpha\beta}, \kappa_\alpha$, $\alpha = 1,2$) and corresponding energy conjugated components of the resultant force and couple vectors ($N^{\alpha\beta}, Q^\alpha, M^{\alpha\beta}, M^\alpha$), respectively. The constants α_i and β_i are defined by the equations AE45.

Following Cowin [10] (compare also [11-12]) we set $\mu \equiv \mu - \frac{1}{2}\kappa$ and we rewrite equations AE45 as

$$
\alpha_1 = \tilde{\lambda}h = \frac{Ev}{1-v^2}h, \qquad \tilde{\lambda} = \frac{2\mu\lambda}{2\mu+\lambda} = \frac{Ev}{1-v^2}, \qquad \mu = \frac{E}{2(1+v)},
\tag{2}
$$

$$
\alpha_2 = (\mu - \tfrac{1}{2}\kappa)h,
\tag{3}
$$

$$
\alpha_3 = (\mu + \tfrac{1}{2}\kappa)h,
\tag{4}
$$

$$
\alpha_4 = (\mu + \tfrac{1}{2}\kappa)h,
\tag{5}
$$

$$
\beta_1 = \alpha h - (\mu - \tfrac{1}{2}\kappa)\frac{h^3}{12},
\tag{6}
$$

$$
\beta_2 = \beta h - \tfrac{1}{12}\tilde{\lambda}h^3,
\tag{7}
$$

$$
\beta_3 = \gamma h - \tfrac{1}{12}(2\mu+\tilde{\lambda})h^3,
\tag{8}
$$

$$
\beta_4 = \gamma h.
\tag{9}
$$

It is seen that to fully describe the above coefficients six elastic constants are necessary; (the same number of elastic constants has been identified for shells in [13]). Two of them are classical Lame parameters λ and μ (or equivalently the technical constants E and v). The remaining four constants are interconnected with four scalar parameters defined as follows (compare AE, Table 1):

$$
N^2 = \frac{\kappa}{2\mu+\kappa} \Rightarrow \kappa = 2\mu\frac{N^2}{1-N^2}, \quad 0 < N < 1,
\tag{10}
$$

$$
l_b^2 = \frac{\gamma}{4\mu} \Rightarrow \gamma = 4\mu l_b^2,
\tag{11}
$$

$$l_t^2 = \frac{\beta + \gamma}{2\mu} \Rightarrow \beta = 2\mu l_t^2 - \gamma, \tag{12}$$

$$\Psi = \frac{\beta + \gamma}{\alpha + \beta + \gamma} \Rightarrow \alpha = (\beta + \gamma)\left(\frac{1-\Psi}{\Psi}\right) = 2\mu l_t^2\left(\frac{1-\Psi}{\Psi}\right), \ 0 < \Psi \le \frac{3}{2}. \tag{13}$$

Since the equation (1) is decoupled, for sake of brevity we consider here the equivalence of blocks of the generalized strains $\varepsilon_{\alpha\beta}, \varepsilon_\alpha$ conjugated with the stress resultants $N^{\alpha\beta}, Q^\alpha$, the and generalized curvatures and $\kappa_{\alpha\beta}, \kappa_\alpha$ conjugated with the stress couple resultants $M^{\alpha\beta}, M^\alpha$.

2.2. Force stress resultants

From AE16 follows the equivalence between the constants α_i from [1] and that used in constitutive relations considered in [5-8]. The equivalence is recapitulated in Table 1.

Table 1. Relations between constants α_i of Altenbach & Eremeyev and Chróścielewski et al.

Altenbach & Eremeyev [1]	Chróścielewski et al [5][6][7][8]	
$\alpha_1 = \tilde{\lambda}h = \frac{Ev}{1-v^2}h$	$\alpha_1 = Cv = \frac{Ev}{1-v^2}h \equiv \tilde{\lambda}h, \ C = \frac{Eh_0}{1-v^2}$	(14)
$\alpha_2 = (\mu - \frac{1}{2}\kappa)h$	$\alpha_2 = 0$	(15)
$\alpha_3 = (\mu + \frac{1}{2}\kappa)h,$ $\alpha_3 = 2\mu h = 2\frac{E}{2(1+v)}h = \frac{E}{(1+v)}h$	$\alpha_3 = C(1-v) = \frac{E(1-v)}{1-v^2}h = \frac{Eh}{1+v} = 2\mu h$	(16)
$\alpha_4 \equiv \alpha_3 = (\mu + \frac{1}{2}\kappa)h = 2\mu h$	$\alpha_4 = \alpha_s \frac{1}{2}C(1-v) = \alpha_s \frac{1}{2}\frac{E(1-v)}{1-v^2}h = \alpha_s \frac{Eh}{2(1+v)} = \alpha_s \mu h$	(17)

It may be noted that the factor $\frac{1}{2}$ appears in the relations (17) which follows from the fact that the shell theory is formulated in terms of engineering shear strains.

The value of the shear correction factor α_s has been a topic of numerous analyses. Its physical sense on the grounds of mechanics of beams, plates and shells is well recognized. Typical values of α_s are known and oscillate about 1. For plates and shells, α_s varies between $\pi^2/12$ to 1 (usually $\alpha_s = \frac{5}{6}$, cf. for instance [14], [15]). For detailed information cf. for instance [16].

From (15) it is seen that α_2 defined by (3) vanishes in the shell constitutive equations used in [5-8]. In connection with (3) and (10) it may easily be shown that

$$\alpha_2 = 0 \quad \Leftrightarrow \quad N = \frac{\sqrt{2}}{2}. \tag{18}$$

With (18) we may generalize the constants in the shell constitutive equations for the stress resultants by writing them in terms of polar ratio (10). Starting from (1) and using the expressions (14), (15), (16), (17) we show that

$$\begin{Bmatrix} N^{11} \\ N^{22} \\ N^{12} \\ N^{21} \\ Q^1 \\ Q^2 \end{Bmatrix} = h \begin{bmatrix} \frac{E}{1-v^2} & \frac{vE}{1-v^2} & & & & \\ \frac{vE}{1-v^2} & \frac{E}{1-v^2} & & & & \\ & & \frac{\mu}{1-N^2} & \frac{\mu(1-2N^2)}{1-N^2} & & \\ & & \frac{\mu(1-2N^2)}{1-N^2} & \frac{\mu}{1-N^2} & & \\ & & & & \frac{\mu}{1-N^2} & \\ & & & & & \frac{\mu}{1-N^2} \end{bmatrix} \begin{Bmatrix} \varepsilon_{11} \\ \varepsilon_{22} \\ \varepsilon_{12} \\ \varepsilon_{21} \\ \varepsilon_1 \\ \varepsilon_2 \end{Bmatrix}. \tag{19}$$

Specifying (19) for $N = \frac{\sqrt{2}}{2}$, we obtain

$$\begin{Bmatrix} N^{11} \\ N^{22} \\ N^{12} \\ N^{21} \\ Q^1 \\ Q^2 \end{Bmatrix} = h \begin{bmatrix} \frac{E}{1-v^2} & \frac{vE}{1-v^2} & & & & \\ \frac{vE}{1-v^2} & \frac{E}{1-v^2} & & & & \\ & & 2\mu & 0 & & \\ & & 0 & 2\mu & & \\ & & & & 2\mu & \\ & & & & & 2\mu \end{bmatrix}_{N=\frac{\sqrt{2}}{2}} \begin{Bmatrix} \varepsilon_{11} \\ \varepsilon_{22} \\ \varepsilon_{12} \\ \varepsilon_{21} \\ \varepsilon_1 \\ \varepsilon_2 \end{Bmatrix} = \begin{bmatrix} C & Cv & & & & \\ Cv & C & & & & \\ & & C(1-v) & 0 & & \\ & & 0 & C(1-v) & & \\ & & & & C(1-v) & \\ & & & & & C(1-v) \end{bmatrix}_{N=\frac{\sqrt{2}}{2}} \begin{Bmatrix} \varepsilon_{11} \\ \varepsilon_{22} \\ \varepsilon_{12} \\ \varepsilon_{21} \\ \varepsilon_1 \\ \varepsilon_2 \end{Bmatrix}. \tag{20}$$

Thus we have shown that the shell constitutive equations for the stress resultants used in [5-8] are equivalent to the constitutive equations of the micropolar plates from [1] by letting $N = \frac{\sqrt{2}}{2}$.

2.3. Stress couple resultants

The equation AE16 furnishes also equivalence relations for the part of constitutive equations associated with the couple resultants. These relations are repeated here in Table 2.

Table 2. Relations between constants β_i of Altenbach & Eremeyev and Chróscielewski et al.

Altenbach & Eremeyev [1]	Chróscielewski et al. [5-8]	
$\beta_1 = \alpha h - (\mu - \frac{1}{2}\kappa)\frac{h^3}{12}$	$\beta_1 = Dv = \frac{Eh^3}{12(1-v^2)}v = \frac{1}{12}Cvh^2$ $= \frac{1}{12}\frac{2\mu h}{(1-v)}vh^2 = 2\mu h \frac{vh^2}{12(1-v)}$	(21)
$\beta_2 = \beta h - \tilde{\lambda}\frac{h^3}{12}$	$\beta_2 = 0$	(22)
$\beta_3 = \gamma h - (2\mu + \tilde{\lambda})\frac{h^3}{12}$	$\beta_3 = D(1-v) = \frac{Eh^3}{12(1+v)} = 2\mu h \frac{1}{12}h^2$	(23)
$\beta_4 = \gamma h$	$\beta_4 = \alpha_t \frac{1}{2}D(1-v) = \alpha_t \frac{1}{2}\frac{Eh^3}{12(1+v)} =$ $\alpha_t \frac{h^3}{12}\frac{E}{2(1+v)} = \mu h \alpha_t \frac{h^2}{12}$	(24)

Rewriting the relation (23)$_1$ from [1] in terms of (11) we obtain the following relation:

$$\beta_3 = 2\mu h \left(2l_b^2 - \frac{1}{12}\frac{1}{1-v}h^2\right) \equiv 2\mu h \frac{1}{12}h^2, \tag{25}$$

which in turn gives the formula for l_b

$$2l_b^2 - \frac{1}{12}\frac{1}{1-v}h^2 \equiv \frac{1}{12}h^2 , \quad l_b^2 = \frac{1}{24}\frac{2-v}{1-v}h^2 , \quad \frac{l_b^2}{h^2} = \frac{1}{24}\frac{2-v}{1-v} . \tag{26}$$

Next comparing the equations (24) and using (11) we arrive at

$$\beta_4 = 2\mu h l_b^2 \equiv 2\mu h\alpha_t \frac{1}{24}h^2 , \quad l_b^2 = \frac{1}{24}\alpha_t h^2 , \quad \alpha_t = 24\frac{l_b^2}{h^2} . \tag{27}$$

From the relations (22) it follows that

$$\beta_2 = 2\mu h(l_t^2 - 2l_b^2) - \frac{1}{12}2\mu\frac{v}{1-v}h^3 = 2\mu h\left((l_t^2 - 2l_b^2) - \frac{1}{12}\frac{v}{1-v}h^2\right) \equiv 0 \tag{28}$$

Hence

$$l_t^2 = 2l_b^2 + \frac{1}{12}\frac{v}{1-v}h^2 = (\frac{1}{12}\frac{2-v}{1-v} + \frac{1}{12}\frac{v}{1-v})h^2 = \frac{1}{6}\frac{1}{1-v}h^2 , \quad l_t^2 = \frac{1}{6(1-v)}h^2 , \quad l_t^{-2} = \frac{6(1-v)}{h^2} \tag{29}$$

Finally from $(21)_1$ we have

$$\beta_1 = 2\mu h l_t^2 \frac{1-\Psi}{\Psi} - \frac{1}{12}\alpha_2 h^2 = 2\mu h l_t^2 \frac{1-\Psi}{\Psi} - \frac{1}{12}\mu h\frac{1-2N^2}{1-N^2}h^2 = 2\mu h\left(\frac{1-\Psi}{\Psi}l_t^2 - \frac{1}{2}\frac{1-2N^2}{1-N^2}\frac{1}{12}h^2\right) \tag{30}$$

which compared to $(21)_2$ yields

$$\beta_1\big|_{N=\frac{\sqrt{2}}{2}} = 2\mu h l_t^2 \frac{1-\Psi}{\Psi} \equiv Dv = 2\mu h\frac{vh^2}{12(1-v)} , \quad l_t^2 \frac{1-\Psi}{\Psi} \equiv \frac{1}{12}h^2\frac{v}{1-v} , \quad \Psi = \frac{2}{2+v} \tag{31}$$

The relation $\beta_1 + \beta_2 + \beta_3$ from (1) is

$$\beta_1 + \beta_2 + \beta_3 = \alpha h - \frac{1}{12}(\mu - \frac{1}{2}\kappa)h^3 + \beta h - \frac{1}{12}\tilde{\lambda}h^3 + \gamma h - \frac{1}{12}(2\mu + \tilde{\lambda})h^3 = 2\mu\frac{1}{\Psi}l_t^2 h - \frac{1}{12}\mu(\frac{1-2N^2}{1-N^2} + \frac{2(1+v)}{1-v})h^3 \tag{32}$$

which under

$$N = \frac{\sqrt{2}}{2} , \quad l_t^2 = \frac{1}{6}\frac{1}{1-v}h , \quad \Psi = \frac{2}{2+v} \tag{33}$$

yields

$$\beta_1 + \beta_2 + \beta_3\big|_{\Psi=\frac{2}{2+v}, l_t^2=\frac{1}{6}\frac{1}{1-v}h^2, N=\frac{\sqrt{2}}{2}} = 2\mu\frac{2+v}{2}\frac{1}{6}\frac{1}{1-v}h^2 h - \frac{1}{12}\mu(\frac{1-2(\frac{\sqrt{2}}{2})^2}{1-(\frac{\sqrt{2}}{2})^2} + \frac{2(1+v)}{1-v})h^3 = 2\mu\frac{1}{1-v}\frac{1}{12}h^3 = D \tag{34}$$

Finally, the matrix form of (1) for the couple resultants is

$$\begin{Bmatrix} M^{11} \\ M^{22} \\ M^{12} \\ M^{21} \\ M^1 \\ M^2 \end{Bmatrix} = 2Gh \begin{bmatrix} \frac{1}{\Psi}l_t^2 - \frac{1}{12}(\frac{1}{2}\frac{1-2N^2}{1-N^2} + \frac{1+v}{1-v})h^2 & \frac{1-\Psi}{\Psi}l_t^2 - \frac{1}{2}\frac{1-2N^2}{1-N^2}\frac{1}{12}h^2 & 0 & 0 & 0 & 0 \\ & \frac{1}{\Psi}l_t^2 - \frac{1}{12}(\frac{1}{2}\frac{1-2N^2}{1-N^2} + \frac{1+v}{1-v})h^2 & 0 & 0 & 0 & 0 \\ & & 2l_b^2 - \frac{1}{12}\frac{1}{1-v}h^2 & l_t^2 - 2l_b^2 - \frac{1}{12}\frac{v}{1-v}h^2 & 0 & 0 \\ & & & 2l_b^2 - \frac{1}{12}\frac{1}{1-v}h^2 & 0 & 0 \\ & Sym. & & & 2l_b^2 & 0 \\ & & & & & 2l_b^2 \end{bmatrix} \begin{Bmatrix} \kappa_{11} \\ \kappa_{22} \\ \kappa_{12} \\ \kappa_{21} \\ \kappa_1 \\ \kappa_2 \end{Bmatrix} \tag{35}$$

By appealing now to (25) and (33) equation (35) may be rewritten as

$$\begin{Bmatrix} M^{11} \\ M^{22} \\ M^{12} \\ M^{21} \\ M^1 \\ M^2 \end{Bmatrix} = \begin{bmatrix} D & Dv & 0 & 0 & 0 & 0 \\ & D & 0 & 0 & 0 & 0 \\ & & D(1-v) & 0 & 0 & 0 \\ & & & D(1-v) & 0 & 0 \\ Sym. & & & & \alpha_t D(1-v) & 0 \\ & & & & & \alpha_t D(1-v) \end{bmatrix} \begin{Bmatrix} \kappa_{11} \\ \kappa_{22} \\ \kappa_{12} \\ \kappa_{21} \\ \kappa_1 \\ \kappa_2 \end{Bmatrix} \tag{36}$$

which is exactly the same as that used in e.g. [5-8].

3. Numerical examples

Using in (27) the relation (26) we arrive at the fundamental formula for the coefficient α_t which is the necessary condition of the equivalence between Altenbach an Eremeyev [1] constitutive relations and those of Chróścielewski et al. [5-8]

$$\alpha_t = \frac{2-v}{1-v} \qquad (37)$$

Equation (37) represents a hyperbola, depicted in Fig. 1, bounded by two asymptotes: $\alpha_t = 1$ and $v = 1$. Relation (37) shows clearly that α_t is material constant dependent on Poisson's ratio. It should not be confused with 'penalty multiplier' as in [17] or [18].

From (37) it follows that for typical values $v \in [0; 0.5]$ one obtains $\alpha_t \in [2,3]$. The values of α_t so estimated are greater than those usually used in numerical simulations presented, among others, in [5-8]. Therefore in structures where the membrane stiffness plays an important role in deformation we may expect some α_t-locking. This issue is pursued further in this section. Summarizing some results from [5-8] we present here representative examples that show the influence of α_t on numerical results. The analysis is confined to the linear range of deformations. To avoid discussions about a mesh convergence, spurious zero-energy forms or satisfaction of a patch-test, we use 16-node CAM finite elements [5-8] with full integration (FI) in all numerical simulations.
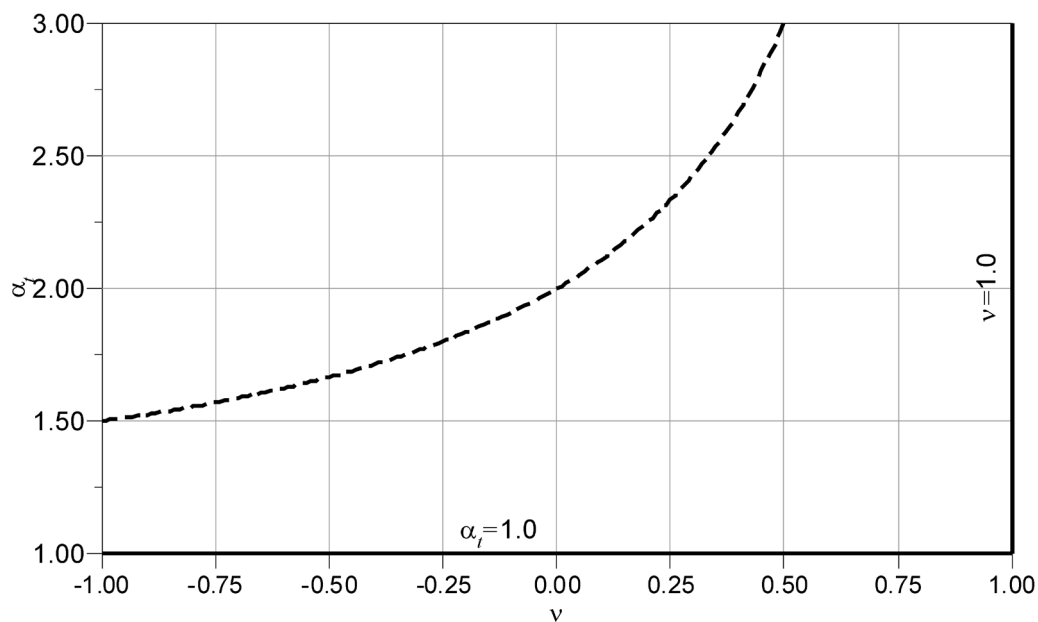

Fig. 1. Nonlinear dependence of α_t on v

3.1. L-shaped frame in plane stress

Consider an L-shaped frame in plane (micropolar) stress as shown in Fig. 2. This example has been studied, among others, in [7] and is motivated by the cantilever L-shaped plate studied, among others, in [19], [20]. The structure is clamped at the bottom end and is loaded with the moment M applied at the point (a). Since the moment M is energy conjugated with drilling degree of freedom this example can not be solved using standard plane stress formulations ot the standard five-parameter Reissner type shell theory. In computations, following [19] we use the data: $L = 240\,mm$, $b = 30\,mm$, $h_0 = 0.6\,mm$, $E = 71240\,N/mm^2$, $v = 0.31$. The value

of the loading moment $M = 0.001 \cdot M_{ref}$, where $M_{ref} = \dfrac{2\pi EJ}{2L} = 1258914.7 \, Nmm$ is found assuming the pure

bending in $x - y$ plane and the bending stiffness $EI_y(s) = const$.
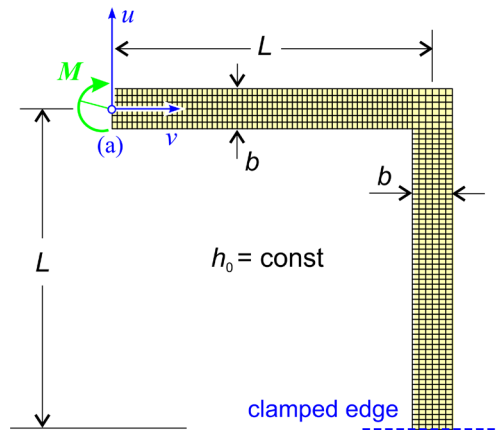

Fig. 2. L-shaped frame, concept of discretization, geometry and loads

In comparison with the results presented in [7], we use finer discretization: 4 elements (16-node CAM, FI) along the shorter edge of the frame and 40 elements along longer edge plus additionally 16 elements for the corner zone. This amounts to the total of 3328 nodes and 9945 active equations. Following the approach presented in [5-7] we have studied the influence of α_t on the values of displacements of the point (a). The results are presented in Fig. 3. The curves are normalized by the values of displacements for $\alpha_t = 0.01$ given in Table 3. For comparison, we also present the values due to α_t found from (37) for $v = 0.31$.
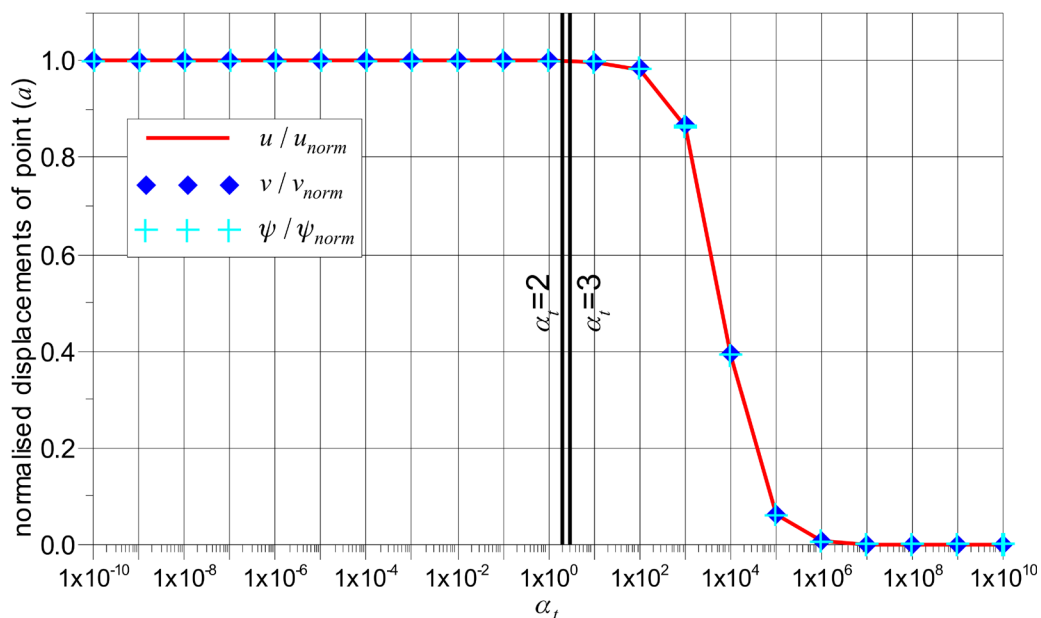

Fig. 3. L-shaped frame, influence of α_t on values of displacements of the point (a)

Table 3. L-shaped frame, values of displacements

	u [mm]	v [mm]	ψ

$\alpha_t = 0.01$	1.10454	0.377792	0.00617377
$\alpha_t = 2.449$ (37) $v = 0.31$	1.09657	0.377628	0.00615710

3.2. Simply supported channel beam

A simply supported channel beam loaded with uniformly distributed load [7] (cf. Fig. 4) can be traced back to the early work of Lee and Harris [21] (see also [22] for large displacement elasto-plastic analysis). The geometry is described by $L = 36$ in, $a = 2$ in, $b = 6$ in, $h = 0.05$ in. The load is $p = 100$ lb/in while the material constants are $E = 10^7$ lb/in and $v = 0.333$. In computations we exploit symmetry of the structure. A mesh consisting of 4 elements (16-node CAM, FI) for each flange, 8 elements for web and 24 elements for half of the beam length has been used, which yields 3577 nodes and 21240 active equations. In computations we have studied displacements of the point (a). Similarly to the previous example, the reference values of displacements for $\alpha_t = 0.01$ are presented in Table 4 while Fig. 5 shows the respective curves, normalized by values for $\alpha_t = 0.01$ given in Table 4.
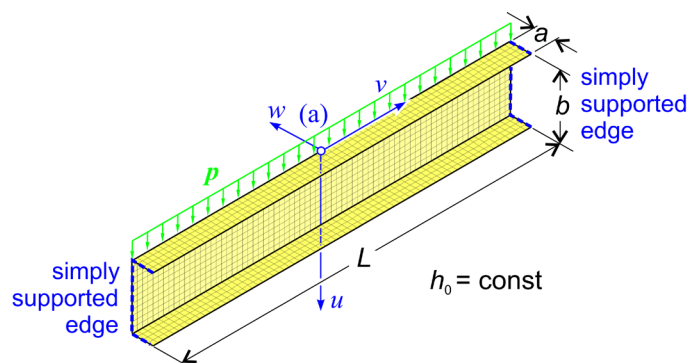

Fig. 4. Simply supported channel beam, geometry and load

Table 4. Simply supported channel beam, values of displacements of the point (a)

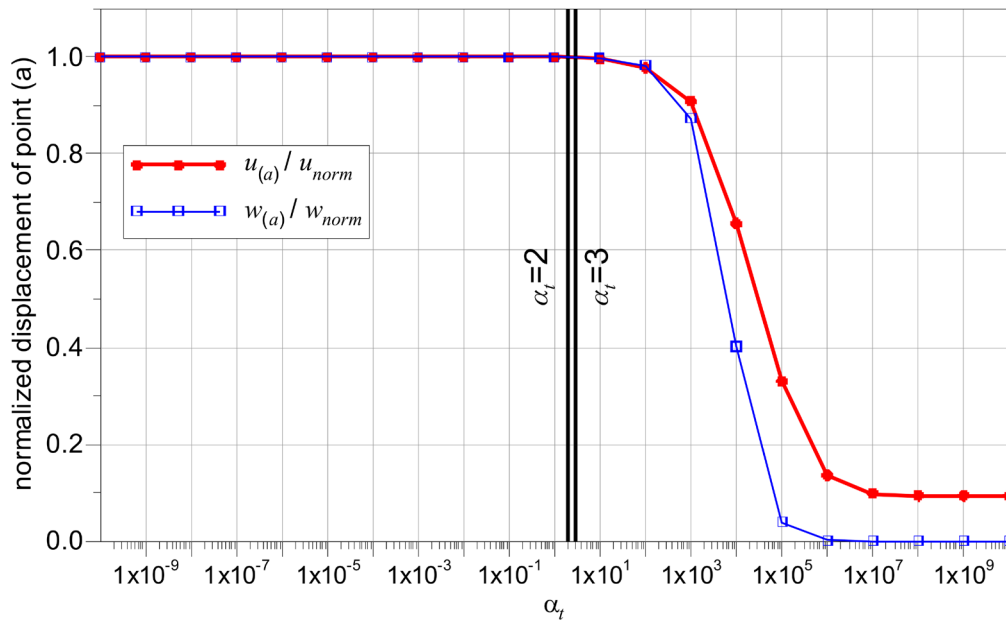|	u [in]	w [in]
$\alpha_t = 0.01$	0.198134	0.369642
$\alpha_t = 2.499$ (37) $v = 0.333$	0.197927	0.369434

Fig. 5. Simply supported channel beam, influence of α_t on values of displacements of the point (a).

3.3. Three intersecting plates

Following [23] we analyze the static version (cf. Fig. 6) of the challenging problem of dynamics of three intersecting plates proposed in [24]. The curious question of this example is that the results reported in the literature are considerably different, though the same geometry and material seem to be used, see discussion in [9]. The material properties are $E = 2 \times 10^7$, $v = 0.25$. In comparison with original formulation we modify here the thickness of the plates to $h_0 = const = 0.5$. The load is $P = 1$. The mesh used in computations consisted of 4 elements (16-node CAM, FI) for each shorter edge of the plate and 12 elements along the longer edge. It yields 1417 nodes and 8346 active equations. The reference displacements and rotations of point the (a) are set in Table 5, while Fig. 7 portrays the dependence of computed values on α_t. The graph is normalized by values of (generalized) displacements for $\alpha_t = 0.01$ given in Table 5

Table 5. Three intersecting plates, values of displacements of the point (a)

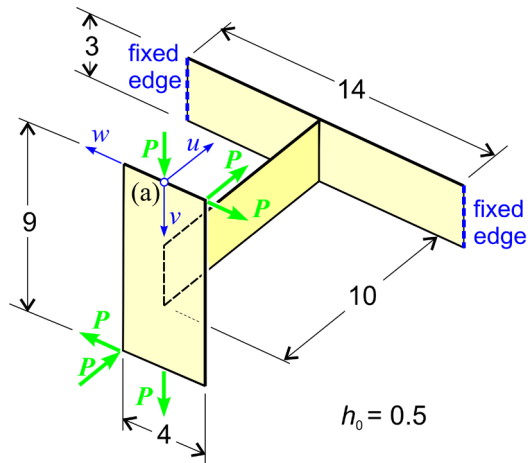|	u	v	w	φ_1	φ	φ_3
$\alpha_t = 0.01$	-7.2857×10^{-4}	1.505×10^{-3}	-1.97×10^{-4}	1.2919×10^{-4}	7.6008×10^{-5}	-1.6447×10^{-4}
$\alpha_t = 2.3(3)$ (37) $v = 0.25$	-7.28568×10^{-4}	1.50495×10^{-3}	-1.97004×10^{-4}	1.2919×10^{-4}	7.6008×10^{-5}	-1.6447×10^{-4}

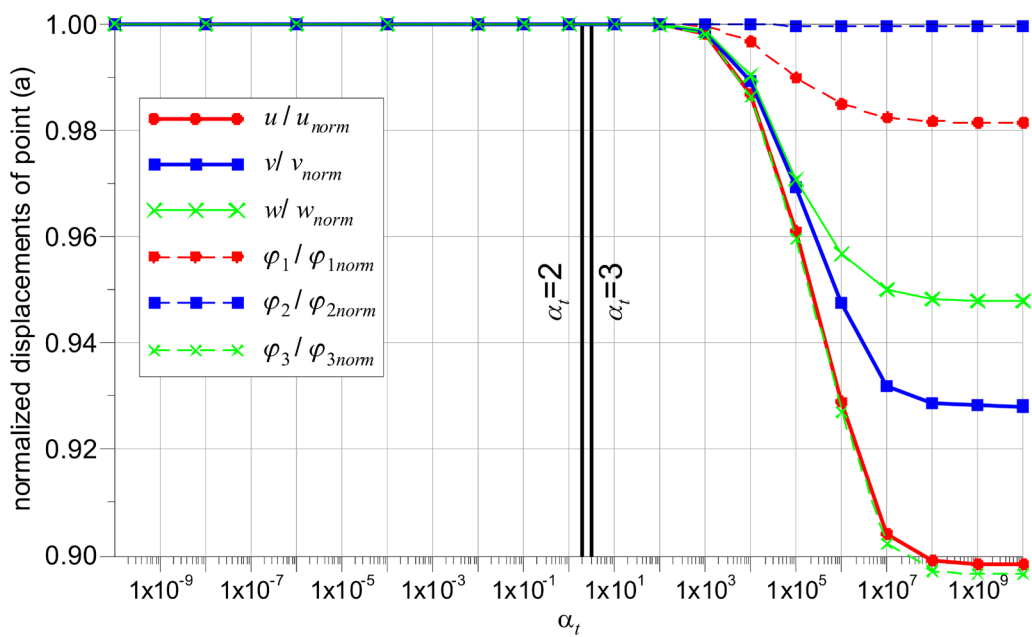Fig. 6. Three intersecting plates, geometry and loads

Fig. 7. Three intersecting plates, influence of α_t on values of displacements of the point (a).

4. Conclusions

The present and other studies from [5-7] indicate that for $10^{-10} \leq \alpha_t \leq 10^{+10}$ there exist three clearly pronounced ranges of influence of α_t. In the most important from the computational viewpoint $\alpha_t \in [10^{-10}; \approx 0.01]$, α_t does not affect the deformation and differences in computed deflections are negligible.

In the transient range $\alpha_t \in [0.1; 10^{+7}]$ with the growth of α_t the values of displacements tend to decrease. This effect is clearly observable already for $\alpha_t \approx 10$. Therefore the value of α_t found from (37) becomes almost the upper bound of the transient range. This bound depends on the analyzed structure. The last range may be described as $\alpha_t > 10^{+7}$.

In the two latter ranges, a quantitative different character of influence of α_t on the overall behavior of the structure is visible. In case of membrane dominated situations (example 1 and 2) the values of $\alpha_t > 10^{+3}$ cause vanishing of the deformation. Such case is referred to as the α_t-locking. In case of bending dominated case (example 3) for $\alpha_t > 10^{+3}$ there appears a stabilization of displacements on slightly lower level when compared with the solutions from the first range.

The above results support the main conclusions:

1) The presented results confirm that the Altenbach and Eremeyev model and the shell constitutive equations are equivalent under some values of parameters. Yet, the search for constitutive models for micropolar plates and shells should still be pursued so that the resulting value of α_t would drop below 3 (or even below 1), at least for materials that do not exhibit micropolar characteristics.

2) Assuming that the equivalence between two models holds, it is possible to assess the values of four material constants of the micropolar plate based only on E and v.

3) The presented numerical simulations show that the bounds on the value of α_t result in almost 'locked' solution. Since the observed effect is not strictly caused by FEM methodology we propose to refer to it as to α_t-locking.

References

[1] H. Altenbach and V. A. Eremeyev, On the linear theory of micropolar plates. Z. Angew. Math. Mech. **89**(4), 242–256 (2009) / **DOI** 10.1002/zamm.200800207.

[2] W. Pietraszkiewicz and V. Eremeyev, On natural strain measures of the non-linear micropolar continuum, International Journal of Solids and Structures, **46**, 774–787 2009.

[3] S. Ramezani, R. Naghdabadi and S. Sohrabpoura, Constitutive equations for micropolar hyper-elastic materials, International Journal of Solids and Structures, **46**(14-15), 2765-2773 2009.

[4] A. Libai and J.G, Simmonds, The Nonlinear Theory of Elastic Shells. Cambridge University Press, 1998

[5] J. Chróścielewski, J. Makowski and H. Stumpf, Genuinely resultant shell finite elements accounting for geometric and material non-linearity, International Journal for Numerical Methods in Engineering, **35**, 63–94 1992.

[6] J. Chróścielewski, J. Makowski and H. Stumpf, Finite element analysis of smooth, folded and multi-shell structures, Comp. Meth. Appl. Mech. Engng., **41**, 1–46 1997.

[7] J. Chróścielewski, J. Makowski and W. Pietraszkiewicz, Statics and Dynamics of Multifold Shells: Nonlinear Theory and Finite Element Method, (in Polish), Institute of Fundamental Technological Research Press, Warsaw, 2004.

[8] J. Chróścielewski and W. Witkowski, 4-node semi-EAS element in 6–field nonlinear theory of shells, International Journal for Numerical Methods in Engineering, **68**, 1137–1179 2006, DOI: 10.1002/nme.1740.

[9] J. Chróścielewski and W. Witkowski, Discrepancies of energy values in dynamics of three intersecting plates, Commun. Numer. Meth. Engng., 2008, DOI: 10.1002/cnm.1208.

[10]   S. C. Cowin, An incorrect inequality in micropolar elasticity theory, J. Appl. Mech. Phys., **21**, 494–497 1970.

[11]   S. C. Cowin, Stress functions for Cosserat elasticity, Int. J. Solids Structures, **6**, 389–398 1970.q

[12]   W. Nowacki, Theory of asymmetric elasticity, Pergamon Press, Oxford, 1986.

[13]   V.A. Eremeyev and W. Pietraszkiewicz, Local symmetry group in the general theory of elastic shells, Journal of Elasticity, **85**, 125–152 2006.

[14]   T.J.R Hughes, The Finite Element Method: linear static and dynamics finite element analysis. Dover Publications, Inc., Mineola, New York 2000.

[15]   K. Wiśniewski, A shell theory with independent rotations for relaxed Biot stress and right stretch strain, Computational Mechanics **21**, 101–122, 1998

[16]   G Jemielita, Teorie płyt sprężystych. W: Cz. Woźniak (Ed.), Mechanika sprężystych płyt i powłok, cz. III, 143-330. Wyd. Nauk. PWN, Warszawa 2001 (in Polish).

[17]   R. Eberlein and P. Wriggers, Finite element concepts for finite elastoplastic strain and isotropic stress response in shells: theoretical and computational analysis. Comp. Meth. Appl. Mech. Engng, **171**, 243–279, 1999.

[18]   X.G. Tan, L. Vu-Quoc, Efficient and accurate multilayer solid-shell element: Non-linear materials at finite strain, International Journal for Numerical Methods in Engineering, **63**, 2124–2170, 2005, DOI: 10.1002/nme.1360.

[19]   Argyris J.H., Dunne P.C., Malejannakis G.A. and E. Scharpf E, On large displacement - small strain analysis of structures with rotational degrees of freedom, Comp. Meth. Appl. Mech. Engng, 15, 99–135 1978.

[20]   P. Wriggers and F. Gruttmann, [1993], Thin shells with finite rotations formulated in Biot stresses: Theory and finite element formulation. International Journal for Numerical Methods in Engineering 36, 2049–2071 1993.

[21]   H. P. Lee and P. J. Haris, Post-buckling strength of thin-walled members, Computers and Structures, **10**, 689–702, 1979.

[22]   J. Chróścielewski, Nonlinear geometric and material FEM analysis of stiffened plates, PhD thesis, Gdansk University of Technology, 1983.

[23]   W. Witkowski, 4-Node combined shell element with semi-EAS-ANS strain interpolations in 6-parameter shell theories with drilling degrees of freedom, Computational Mechanics, **43**, 307–319 2009, DOI 10.1007/s00466-008-0307-x

[24]   J.C. Simo and N. Tarnow, A new energy and momentum conserving algorithm for the non-linear dynamics of shells. International Journal for Numerical Methods in Engineering, **37**, 2527–2549. 1994

Appendix 1. Equation Section (Next)

In what follows all vectors and tensors are referred to Cartesian frame of reference with base vectors $\mathbf{e}_k$, $k = 1, 2, 3$. Definition of the linear strain measures (AE7) is

$$\boldsymbol{\varepsilon} = \nabla^s \mathbf{u} + \mathbf{A} \times \boldsymbol{\theta}, \quad \boldsymbol{\kappa} = \nabla^s \boldsymbol{\theta} \tag{A1}$$

Here $\nabla^s (...) = \mathbf{e}_1 \otimes (...)_{,1} + \mathbf{e}_2 \otimes (...)_{,2}$ and $\mathbf{A} = \mathbf{e}_k \otimes \mathbf{e}_k - \mathbf{e}_3 \otimes \mathbf{e}_3 = \mathbf{e}_1 \otimes \mathbf{e}_1 + \mathbf{e}_2 \otimes \mathbf{e}_2$. The operation $\mathbf{A} \times \boldsymbol{\theta}$ is defined as follows (Eremeyev, private communication)

$$
\begin{aligned}
\mathbf{A} \times \boldsymbol{\theta} &= (\mathbf{e}_1 \otimes \mathbf{e}_1 + \mathbf{e}_2 \otimes \mathbf{e}_2) \times (\theta_1 \mathbf{e}_1 + \theta_2 \mathbf{e}_2 + \theta_3 \mathbf{e}_3) \\
&= \theta_1 \mathbf{e}_1 \otimes \cancel{\mathbf{e}_1 \times \mathbf{e}_1} + \theta_2 \mathbf{e}_1 \otimes \mathbf{e}_1 \times \mathbf{e}_2 + \theta_3 \mathbf{e}_1 \otimes \mathbf{e}_1 \times \mathbf{e}_3 \\
&= \theta_1 \mathbf{e}_2 \otimes \mathbf{e}_2 \times \mathbf{e}_1 + \theta_2 \mathbf{e}_2 \otimes \cancel{\mathbf{e}_2 \times \mathbf{e}_2} + \theta_3 \mathbf{e}_2 \otimes \mathbf{e}_2 \times \mathbf{e}_3 \\
&= \theta_2 \mathbf{e}_1 \otimes \mathbf{e}_3 - \theta_1 \mathbf{e}_2 \otimes \mathbf{e}_3 + \theta_3 (\mathbf{e}_2 \otimes \mathbf{e}_1 - \mathbf{e}_1 \otimes \mathbf{e}_2)
\end{aligned}
\tag{A2}
$$

The displacement gradient in the plane is

$$\nabla^s \mathbf{u} = \mathbf{e}_1 \otimes \mathbf{u}_{,1} + \mathbf{e}_2 \otimes \mathbf{u}_{,2} = \mathbf{e}_1 \otimes (u_{1,1} \mathbf{e}_1 + u_{2,1} \mathbf{e}_2 + u_{3,1} \mathbf{e}_3) + \mathbf{e}_2 \otimes (u_{1,2} \mathbf{e}_1 + u_{2,2} \mathbf{e}_2 + u_{3,2} \mathbf{e}_3) \tag{A3}$$

Therefore the equation (A1) in components read

$$
(\boldsymbol{\varepsilon})_{ij} = \begin{bmatrix} u_{1,1} & u_{2,1} - \theta_3 & u_{3,1} + \theta_2 \\ u_{1,2} + \theta_3 & u_{2,2} & u_{3,2} - \theta_1 \\ 0 & 0 & 0 \end{bmatrix}, \quad
(\boldsymbol{\kappa})_{ij} = \begin{bmatrix} \kappa_{11} & \kappa_{21} & \kappa_{31} \\ \kappa_{12} & \kappa_{22} & \kappa_{32} \\ 0 & 0 & 0 \end{bmatrix} = \begin{bmatrix} \theta_{1,1} & \theta_{2,1} & \theta_{3,1} \\ \theta_{1,2} & \theta_{2,2} & \theta_{3,2} \\ 0 & 0 & 0 \end{bmatrix} \tag{A4}
$$

The term

$$\boldsymbol{\varepsilon}_\square = \boldsymbol{\varepsilon} \mathbf{A} = (\nabla^s \mathbf{u} + \mathbf{A} \times \boldsymbol{\theta}) \mathbf{A} \tag{A5}$$

is evaluated in the following steps.

$$
\begin{aligned}
(\nabla^s \mathbf{u}) \mathbf{A} &= (\mathbf{e}_1 \otimes \mathbf{u}_{,1} + \mathbf{e}_2 \otimes \mathbf{u}_{,2})(\mathbf{e}_1 \otimes \mathbf{e}_1 + \mathbf{e}_2 \otimes \mathbf{e}_2) \\
&= (\mathbf{e}_1 \otimes \mathbf{u}_{,1})(\mathbf{e}_1 \otimes \mathbf{e}_1) + (\mathbf{e}_1 \otimes \mathbf{u}_{,1})(\mathbf{e}_2 \otimes \mathbf{e}_2) + (\mathbf{e}_2 \otimes \mathbf{u}_{,2})(\mathbf{e}_1 \otimes \mathbf{e}_1) + (\mathbf{e}_2 \otimes \mathbf{u}_{,2})(\mathbf{e}_2 \otimes \mathbf{e}_2) \\
&= \mathbf{u}_{,1} \mathbf{e}_1 (\mathbf{e}_1 \otimes \mathbf{e}_1) + \mathbf{u}_{,1} \mathbf{e}_2 (\mathbf{e}_1 \otimes \mathbf{e}_2) + \mathbf{u}_{,2} \mathbf{e}_1 (\mathbf{e}_2 \otimes \mathbf{e}_1) + \mathbf{u}_{,2} \mathbf{e}_2 (\mathbf{e}_2 \otimes \mathbf{e}_2) \\
&= u_{1,1} (\mathbf{e}_1 \otimes \mathbf{e}_1) + u_{2,1} (\mathbf{e}_1 \otimes \mathbf{e}_2) + u_{1,2} (\mathbf{e}_2 \otimes \mathbf{e}_1) + u_{2,2} (\mathbf{e}_2 \otimes \mathbf{e}_2)
\end{aligned}
\tag{A6}
$$

$$
\begin{aligned}
(\mathbf{A} \times \boldsymbol{\theta}) \mathbf{A} &= (\theta_2 \mathbf{e}_1 \otimes \mathbf{e}_3 - \theta_1 \mathbf{e}_2 \otimes \mathbf{e}_3 + \theta_3 (\mathbf{e}_2 \otimes \mathbf{e}_1 - \mathbf{e}_1 \otimes \mathbf{e}_2))(\mathbf{e}_1 \otimes \mathbf{e}_1 + \mathbf{e}_2 \otimes \mathbf{e}_2) = \\
&= -\theta_1 ((\mathbf{e}_2 \otimes \mathbf{e}_3)(\mathbf{e}_1 \otimes \mathbf{e}_1) + (\mathbf{e}_2 \otimes \mathbf{e}_3)(\mathbf{e}_2 \otimes \mathbf{e}_2)) \\
&\quad + \theta_2 ((\mathbf{e}_1 \otimes \mathbf{e}_3)(\mathbf{e}_1 \otimes \mathbf{e}_1) + (\mathbf{e}_1 \otimes \mathbf{e}_3)(\mathbf{e}_2 \otimes \mathbf{e}_2)) \\
&\quad + \theta_3 ((\mathbf{e}_2 \otimes \mathbf{e}_1)(\mathbf{e}_1 \otimes \mathbf{e}_1) + (\mathbf{e}_2 \otimes \mathbf{e}_1)(\mathbf{e}_2 \otimes \mathbf{e}_2) - (\mathbf{e}_1 \otimes \mathbf{e}_2)(\mathbf{e}_1 \otimes \mathbf{e}_1) - (\mathbf{e}_1 \otimes \mathbf{e}_2)(\mathbf{e}_2 \otimes \mathbf{e}_2)) = \\
&= -\theta_1 (\delta_{31}(\mathbf{e}_2 \otimes \mathbf{e}_1) + \delta_{32}(\mathbf{e}_2 \otimes \mathbf{e}_2)) + \theta_2 (\delta_{31}(\mathbf{e}_1 \otimes \mathbf{e}_1) + \delta_{32}(\mathbf{e}_1 \otimes \mathbf{e}_2)) + \\
&\quad + \theta_3 (\delta_{11}(\mathbf{e}_2 \otimes \mathbf{e}_1) + \delta_{12}(\mathbf{e}_2 \otimes \mathbf{e}_2) - \delta_{21}(\mathbf{e}_1 \otimes \mathbf{e}_1) - \delta_{22}(\mathbf{e}_1 \otimes \mathbf{e}_2)) = \\
&= \theta_3 (\mathbf{e}_2 \otimes \mathbf{e}_1 - \mathbf{e}_1 \otimes \mathbf{e}_2)
\end{aligned}
\tag{A7}
$$

Finally (A5) becomes

$$(\boldsymbol{\varepsilon}_{\square})_{ij} = \begin{bmatrix} u_{1,1} & u_{2,1} -\theta_3 & 0 \\ u_{1,2} +\theta_3 & u_{2,2} & 0 \\ 0 & 0 & 0 \end{bmatrix} = \begin{bmatrix} \varepsilon_{11} & \varepsilon_{12} & 0 \\ \varepsilon_{21} & \varepsilon_{22} & 0 \\ 0 & 0 & 0 \end{bmatrix} \tag{A8}$$

The term

$$\boldsymbol{\varepsilon}(\mathbf{e}_3 \otimes \mathbf{e}_3) = (\nabla^s \mathbf{u} + \mathbf{A} \times \boldsymbol{\theta})(\mathbf{e}_3 \otimes \mathbf{e}_3) \tag{A9}$$

is

$$\begin{aligned} \nabla^s \mathbf{u}(\mathbf{e}_3 \otimes \mathbf{e}_3) &= (\mathbf{e}_1 \otimes \mathbf{u}_{,1} + \mathbf{e}_2 \otimes \mathbf{u}_{,2})(\mathbf{e}_3 \otimes \mathbf{e}_3) = (\mathbf{e}_1 \otimes \mathbf{u}_{,1})(\mathbf{e}_3 \otimes \mathbf{e}_3) + (\mathbf{e}_2 \otimes \mathbf{u}_{,2})(\mathbf{e}_3 \otimes \mathbf{e}_3) \\ &= \mathbf{u}_{,1} \mathbf{e}_3 (\mathbf{e}_1 \otimes \mathbf{e}_3) + \mathbf{u}_{,2} \mathbf{e}_3 (\mathbf{e}_2 \otimes \mathbf{e}_3) = u_{3,1} (\mathbf{e}_1 \otimes \mathbf{e}_3) + u_{3,2} (\mathbf{e}_2 \otimes \mathbf{e}_3) \end{aligned} \tag{A10}$$

while $(\mathbf{A} \times \boldsymbol{\theta})(\mathbf{e}_3 \otimes \mathbf{e}_3)$ reads

$$\begin{aligned} (\mathbf{A} \times \boldsymbol{\theta})(\mathbf{e}_3 \otimes \mathbf{e}_3) &= \left(\theta_2 \mathbf{e}_1 \otimes \mathbf{e}_3 - \theta_1 \mathbf{e}_2 \otimes \mathbf{e}_3 + \theta_3 (\mathbf{e}_2 \otimes \mathbf{e}_1 - \mathbf{e}_1 \otimes \mathbf{e}_2)\right)(\mathbf{e}_3 \otimes \mathbf{e}_3) \\ &= -\theta_1 (\mathbf{e}_2 \otimes \mathbf{e}_3)(\mathbf{e}_3 \otimes \mathbf{e}_3) + \theta_2 (\mathbf{e}_1 \otimes \mathbf{e}_3)(\mathbf{e}_3 \otimes \mathbf{e}_3) + \\ &\quad + \theta_3 (\mathbf{e}_2 \otimes \mathbf{e}_1)(\mathbf{e}_3 \otimes \mathbf{e}_3) - \theta_3 (\mathbf{e}_1 \otimes \mathbf{e}_2)(\mathbf{e}_3 \otimes \mathbf{e}_3) \\ &= -\theta_1 \delta_{33} (\mathbf{e}_2 \otimes \mathbf{e}_3) + \theta_2 \delta_{33} (\mathbf{e}_1 \otimes \mathbf{e}_3) + \theta_3 \delta_{13} (\mathbf{e}_2 \otimes \mathbf{e}_3) - \theta_3 \delta_{23} (\mathbf{e}_1 \otimes \mathbf{e}_3) \\ &= -\theta_1 (\mathbf{e}_2 \otimes \mathbf{e}_3) + \theta_2 (\mathbf{e}_1 \otimes \mathbf{e}_3) \end{aligned} \tag{A11}$$

Ultimately (A9) is

$$\left(\boldsymbol{\varepsilon}(\mathbf{e}_3 \otimes \mathbf{e}_3)\right)_{ij} = \begin{bmatrix} 0 & 0 & u_{3,1} +\theta_2 \\ 0 & 0 & u_{3,2} -\theta_1 \\ 0 & 0 & 0 \end{bmatrix} = \begin{bmatrix} 0 & 0 & \varepsilon_{31} \\ 0 & 0 & \varepsilon_{32} \\ 0 & 0 & 0 \end{bmatrix} \tag{A12}$$

Utilizing (A6), $\boldsymbol{\kappa}_{\square} = \boldsymbol{\kappa} \mathbf{A}$ is

$$\boldsymbol{\kappa} \mathbf{A} = \theta_{1,1} \left(\mathbf{e}_1 \otimes \mathbf{e}_1\right) + \theta_{2,1} \left(\mathbf{e}_1 \otimes \mathbf{e}_2\right) + \theta_{1,2} \left(\mathbf{e}_2 \otimes \mathbf{e}_1\right) + \theta_{2,2} \left(\mathbf{e}_2 \otimes \mathbf{e}_2\right), \tag{A13}$$

and

$$(\boldsymbol{\kappa}_{\square})_{ij} = \begin{bmatrix} \theta_{1,1} & \theta_{2,1} & 0 \\ \theta_{1,2} & \theta_{2,2} & 0 \\ 0 & 0 & 0 \end{bmatrix} = \begin{bmatrix} \kappa_{11} & \kappa_{12} & 0 \\ \kappa_{21} & \kappa_{22} & 0 \\ 0 & 0 & 0 \end{bmatrix} \tag{A14}$$

Similarly, based on (A10), $\boldsymbol{\kappa}(\mathbf{e}_3 \otimes \mathbf{e}_3)$ reads

$$\boldsymbol{\kappa}(\mathbf{e}_3 \otimes \mathbf{e}_3) = \kappa_{31}(\mathbf{e}_1 \otimes \mathbf{e}_3) + \kappa_{32}(\mathbf{e}_2 \otimes \mathbf{e}_3) \tag{A15}$$

and

$$\left(\boldsymbol{\kappa}(\mathbf{e}_3 \otimes \mathbf{e}_3)\right)_{ij} = \begin{bmatrix} 0 & 0 & \theta_{3,1} \\ 0 & 0 & \theta_{3,2} \\ 0 & 0 & 0 \end{bmatrix} = \begin{bmatrix} 0 & 0 & \kappa_{31} \\ 0 & 0 & \kappa_{32} \\ 0 & 0 & 0 \end{bmatrix} \tag{A16}$$